ELSEVIER

International Journal of Refractory Metals & Hard Materials 19 (2001) 409–417

International Journal of REFRACTORY METALS & HARD MATERIALS

www.elsevier.com/locate/ijrmhm

Microstructure and properties tailoring of liquid-phase sintered SiC

V.A. Izhevskyi *,[1], L.A. Genova, A.H.A. Bressiani, J.C. Bressiani

Instituto de Pesquisas Energeticas e Nucleares, IPEN – CNEN/SP, C.P. 11049, Pinheiros, Sao Paulo, SP 05542-970, Brazil

Received 5 March 2001; accepted 21 March 2001

Abstract

Silicon carbide (SiC) ceramics of the composition SiC-10 vol% ($AlN–Y_2O_3$) were liquid-phase sintered without application of external pressure in a graphite resistance furnace in Ar atmosphere at 1950°C to high density (up to 98.8%). Contents of α-SiC and β-SiC, as well as the granulometry of the α-SiC used, were varying parameters of the initial compositions, the influence of which on densification, microstructure and phase formation during sintering and post-sintering heat treatments was studied. Evolution of microstructure, in particular of the grain morphology occurring due to transformation-controlled grain growth was followed by SEM. The degree of β-SiC to α-SiC phase transformation was measured by means of quantitative XRD using internal standard technique. Fracture toughness of sintered and annealed materials has been determined by the Vickers indentation method and varied in the range 3.6–5.9 MPa $m^{1/2}$. Mechanisms of material toughening are discussed in terms of known toughening mechanisms with consideration of residual porosity variation. © 2001 Elsevier Science Ltd. All rights reserved.

Keywords: Silicon carbide; Ceramics; Sintering; Microstructure design; In situ reinforcement

1. Introduction

Silicon carbide (SiC) is considered as a promising hard ceramic material for a number of applications. Once sintered to high densities, it presents a unique combination of properties, such as exceptional hardness, high wear resistance, good mechanical strength and others, which are maintained up to high temperatures. Liquid-phase sintering of SiC can be achieved within a temperature range 1800–1900°C [1,2] with the aid of metal oxides, such as Al_2O_3, Y_2O_3, and rare-earth oxides [3–8]. This densification technique lately draws more attention because the materials processed by this method exhibit superior mechanical properties. However, oxides interact with SiC with massive gaseous products formation leading to high weight loss and porosity. As it was suggested by Chia et al. [9], aluminum nitride (AlN) in combination with yttria (Y_2O_3), used as sintering aids yields better results. However, a rather limited amount of research was accomplished until now with $AlN–RE_2O_3$ sintering additives formulation [10–13].

Further improvement of SiC-based materials performance is possible, in particular by means of the so-called in situ toughening or self-reinforcement [6,7]. This approach is viable especially for liquid-phase sintered SiC due to the possibility of achievement of in situ β-SiC to α-SiC phase transformation resulting in a three-dimensional interlocking network of elongated plate-like grains with a minimal amount of intergranular phases [14,15]. This, in turn, leads to mechanical properties improvement, in particular of fracture toughness, akin to silicon nitride, for which it has been shown that large elongated grains increase fracture toughness by crack bridging [16] or crack deflection [17].

In the present work, final microstructure tailoring of liquid-phase sintered silicon carbide ceramics (LPS–SiC) with AlN and Y_2O_3 additives was accomplished. Powders of α-SiC of different granulometries, as well as the content of α-SiC in the starting mixture, were used as factors influencing transformation-controlled grain growth during sintering and post-sintering heat treatment. The fracture toughness was measured and discussed in terms of microstructural parameters and known toughening mechanisms.

* Corresponding author.

[1] Invited scientist, on leave from the Institute for Problems of Materials Science, National Academy of Sciences of Ukraine, Kiev, Ukraine.

PII: S0263-4368(01)00015-4

2. Experimental

Mixtures were prepared from high-purity powders of α-SiC of three different granulometries, the specific surface varying from 5 to 15 to 25 m^2/g (grades UF-0.5, UF-15, and UF-25, respectively, H.C. Starck, Goslar, Germany), β-SiC (grade BF-17, H.C. Stark, Goslar, Germany), AlN (H.C. Starck, Germany, grade C), and Y_2O_3 (>99.98% purity, Aldrich Chemical Company, USA) by attrition milling with alumina milling media in isopropyl alcohol for 4 h at 500 rpm. The total amount of sintering aids was kept constant at 10 vol%. The ratio of α-SiC/β-SiC was a variable parameter, the content of α-SiC chosen as 1 wt%, 5 wt% and 10 wt% relative to the amount of β-SiC. The ratio AlN/Y_2O_3 was kept constant at 3:2, the proportion chosen from the $AlN–Y_2O_3$ phase diagram [18] (see Fig. 1).

The slurry obtained after attrition milling was separated from the milling media by passing through an ASTM 325 sieve and subsequently dried in a vacuum rotaevaporator. The process of drying was then completed in a drying box (48 h, 65°C). Finally, the powder was passed through an ASTM 100 sieve to crush soft conglomerates.

Green bodies in the form of cylindrical pellets 14 mm in diameter and about 20 mm height were prepared by uniaxial pressing at 50 MPa, and cold isostatic pressing at 200 MPa. Sintering and post-sintering heat treatments were accomplished in a gas-pressure furnace (Thermal Technologies, Santa Barbara, USA) with a graphite heating element in Ar atmosphere. The flowchart of the materials processing is presented in Fig. 2.

Starting SiC powders were investigated by means of transmission electron microscopy (TEM) with a JEOL JEM-C transmission electron microscope. Morphology

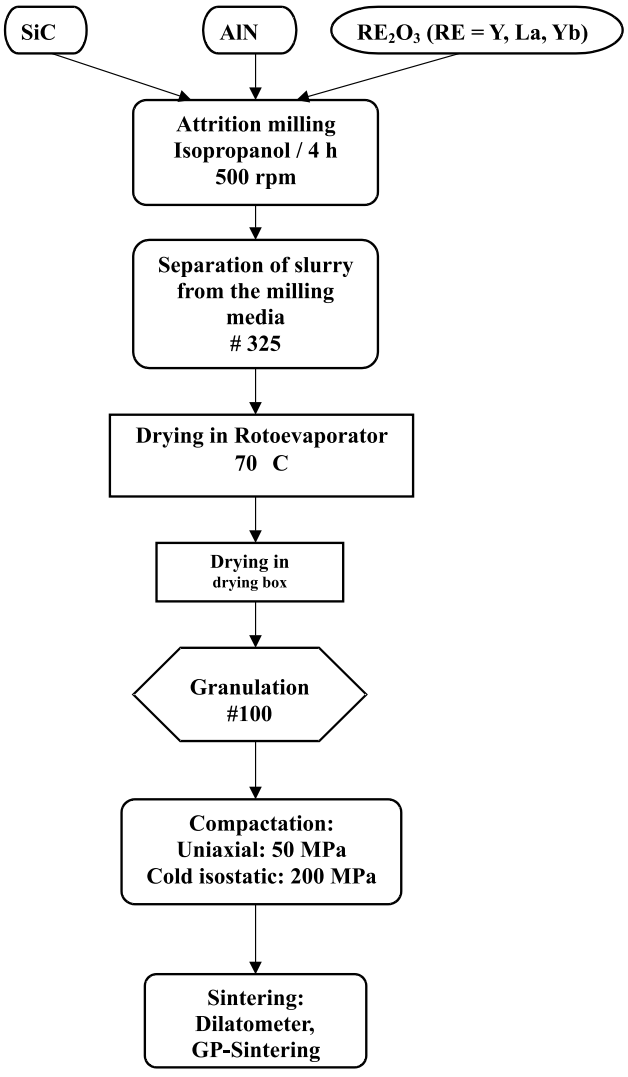

Fig. 2. The flowchart of the materials processing.

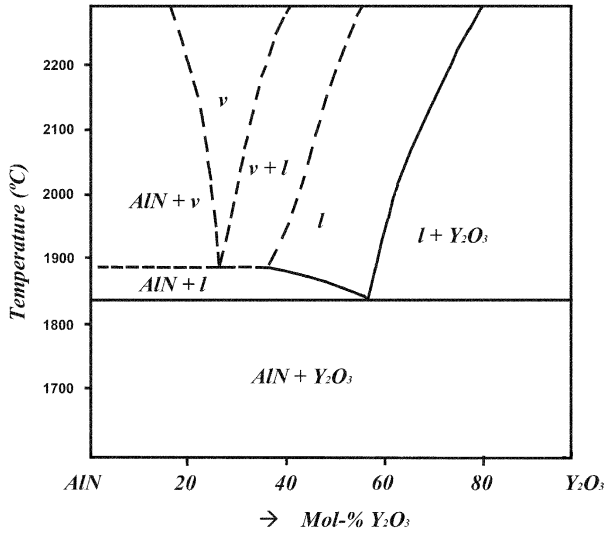

Fig. 1. Behavioral diagram of the $AlN–Y_2O_3$ system [18].

and particle size of various grades of α-SiC were compared for better understanding of phase transformation kinetics and microstructural evolution during sintering and post-sintering heat treatment of materials with different nominal formulations.

Sintered samples were characterized for weight loss, density, phase composition and microstructure. Density was determined by Archimedes method. Phase composition was studied by X-ray diffraction (XRD) on a Siemens D-6000 powder diffractometer (Ni-filtered CuKα radiation, range of detection 10–80° 2Θ). In order to evaluate the phase transformation kinetics, quantitative analysis for α-SiC and β-SiC determination was accomplished by normalizing the sum of the $(111)_{3C}$ and $(006)_{6H}$ reflection intensities using the internal standard method described in detail in the previous work [12]. Microstructure was studied by scanning electron microscopy (SEM) with a Phillips XL-30 elec-

tron microscope with EDS analyzing attachment. Samples for SEM microstructural investigation were prepared by standard ceramographic procedure of multistep grinding and polishing with subsequent chemical etching in Murakami's reagent (10 g of KOH and 10 g of $K_3Fe(CN)_6$ in 50 ml of H_2O at 110°C for 2 to 5 min) for structural elements revelation.

Fracture toughness was measured on surfaces diamond-polished to 1 μm finish by Vickers diamond pyramid indentation in air at contact load of 98 N. Lengths of the surface traces of well-defined radial cracks for eight indentations per sample were measured using an optical microscope with an image analyzing attachment (Omnimet Enterprise, Buehler, USA), and fracture toughness was then calculated according to the method described in [19].

3. Results and discussion

The results of TEM investigation of the starting SiC powders are presented in Fig. 3. As it can be seen, the morphology of the particles of all powders is similar, while the particle size varies significantly. The effect of the grade of the α-SiC used on microstructure formation and β-SiC to α-SiC phase transformation kinetics will be discussed in detail further.

The nomenclature, nominal compositions, and weight loss and relative densities of the prepared materials after sintering are presented in Table 1. The sintering schedule used in the present work (see Fig. 4) was developed based on dilatometric investigations accomplished earlier [12].

As it can be seen, both the final density and the weight loss under the chosen sintering conditions are influenced only slightly by α-SiC content and by the α-SiC powder granulometry in the initial mixture. Densification behavior of thus formulated materials was discussed in detail elsewhere [12,13].

The phase transformation kinetics was studied for all compositions under conditions of post-sintering heat treatment (annealing) at 1950°C under atmospheric argon pressure. The results are presented in Fig. 5. The α-SiC content increases with annealing time for all investigated compositions, however the transformation rate decreases. Even after 16 h, for the majority of the

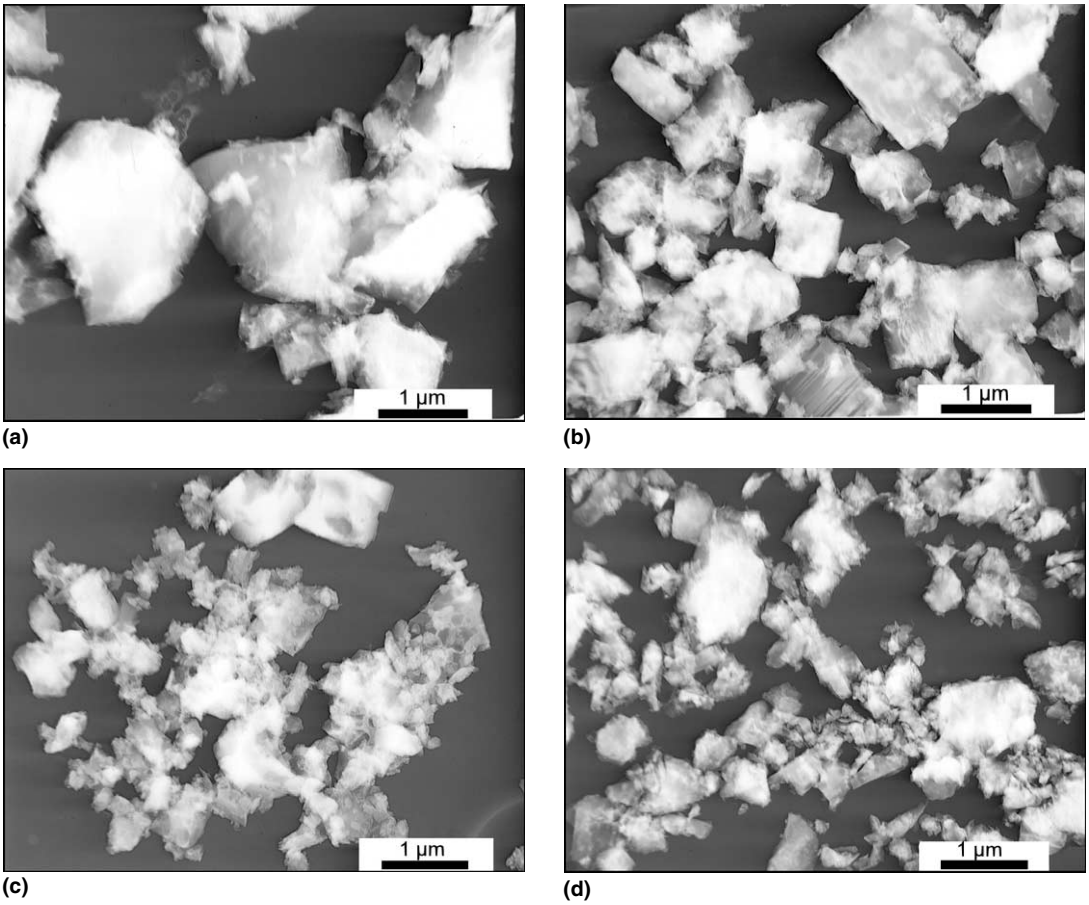

Fig. 3. TEM images of the starting SiC powders: (a) α-SiC, grade UF-05; (b) α-SiC, grade UF-15; (c) α-SiC grade UF-25; (d) β-SiC, grade BF-17.

Table 1
Composition, weight loss and relative densities of as-sintered materials

Material	α-SiC (wt%)			β-SiC (wt%)	Y_2O_3 (wt%)	AlN (wt%)	Weight loss (%)	Relative density (%)
	Grade UF-05	Grade UF-15	Grade UF-25					
SiC1	–	–	0.87	85.58	10.65	2.90	3.41	98.1
SiC5	–	4.32	–	82.13	10.65	2.90	3.21	98.3
SiC5A	–	–	4.32	82.13	10.65	2.90	3.16	98.8
SiC5B	4.32	–	–	82.13	10.65	2.90	3.34	98.2
SiC10	–	8.65		77.80	10.65	2.90	2.99	97.7

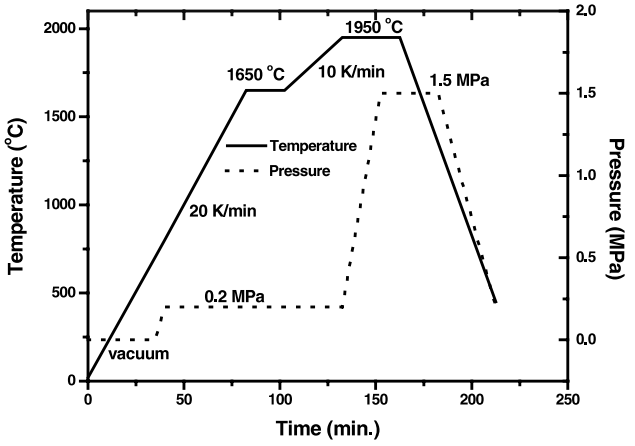

Fig. 4. The time–temperature–gas pressure schedule of the furnace sintering of the materials.

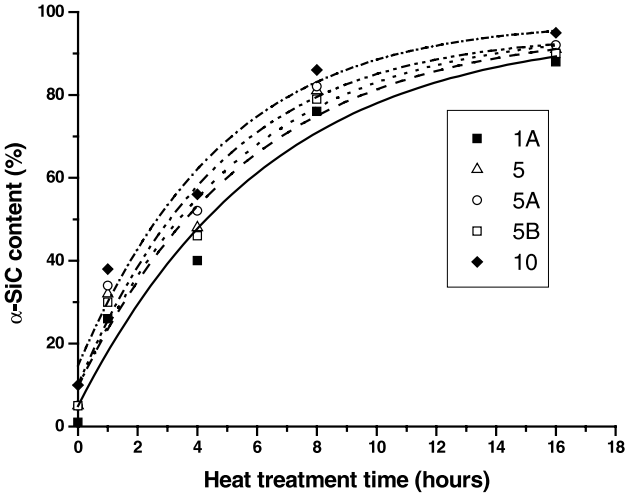

Fig. 5. β-SiC to α-SiC phase transformation kinetics under conditions of annealing at 1950°C under atmospheric Ar pressure.

compositions the transformation was still not complete. The transformation kinetics could be described by a nucleation and grain growth process according to the equation

$$y(t) = a + (b - a)(1 - e^{-kt}),$$

which is the modified version of the equation derived by Christian [20] for grain growth process. y gives the α-SiC content at time (t), a and b are constants for the initial (a) and final (b) α-SiC content; the constant k describes the transformation kinetics. The observed transformation kinetics can be explained by a steric hindrance of grain growth of α-SiC grains. At the initial stages of annealing, α-SiC particles grow without any impediment, resulting in high transformation rates. On the later stages of annealing, the grains come into contact, especially due to a pronounced grain growth anisotropy characterized by high growth rates of the prism planes and low growth rates of the basal planes. Since grain growth becomes hindered, the transformation rate decreases. A somewhat similar behavior has been observed in the case of the α- to β-Si_3N_4 phase transformation [21].

The initial amount of α-SiC in the powder mixtures influences both the kinetics of the transformation, and the degree of transformation. With the increase of the initial α-SiC content, acceleration of the transformation kinetics can be observed (see Fig. 5), and the degree of the transformation increases as well. These results are in good agreement with the ones reported by Nader et al. [14], who reported the absence of β- to α-SiC transformation for compositions based on pure β-SiC powders, and the high amounts of untransformed residual β-SiC for compositions with the β-SiC versus α-SiC content higher than 50%. At the same time both the results of Nader et al., and of the present authors, seem to contradict those of Mulla and Krstic [3], who reported a phase transformation from β-SiC to α-SiC (4H-type) in samples prepared from pure β-SiC powder. However, the different sintering additives, namely high amounts of Al_2O_3, used in [3] may be responsible for such behavior.

It seems to be reasonable to conclude that the presence of α-SiC nucleation sites is required in the investigated system for effective β-SiC to α-SiC phase transformation, and the homogeneous nucleation of α-SiC or the heterogeneous nucleation on β-SiC could be disregarded. Under this assumption the marked influence of the initial α-SiC content on the transformation kinetics can be easily understood since the α-SiC content correlates directly with the number of nucleation sites.

However, the influence of the particle size of the different grades of α-SiC used in the present work seems to be minor. Although some acceleration in β-SiC to α-SiC phase transformation and a higher degree of transformation could be noted, apparently a much finer α-SiC powder would have to be used for sufficient alteration of phase transformation kinetics. It is also possible that the effect of finer α-SiC additions might be more pronounced under lower heat treatment temperatures.

Drawing a parallel with the α to β phase transformation in Si_3N_4 and the role of the liquid phase in the phase transformation process [21–24], it is reasonable to assume that the general trends should be similar for LPS–SiC ceramics. In this regard, the influence of the atmosphere during post-sintering heat treatments of SiC ceramics seems to be a promising issue for further investigation, since the liquid phase, in the majority of cases being a Y_2O_3-rich alumosilicate melt, might be strongly influenced by the atmosphere at sintering temperatures. Until the present time, there is no unanimous opinion on the preferable sintering atmosphere for SiC. Some authors report better results after sintering in

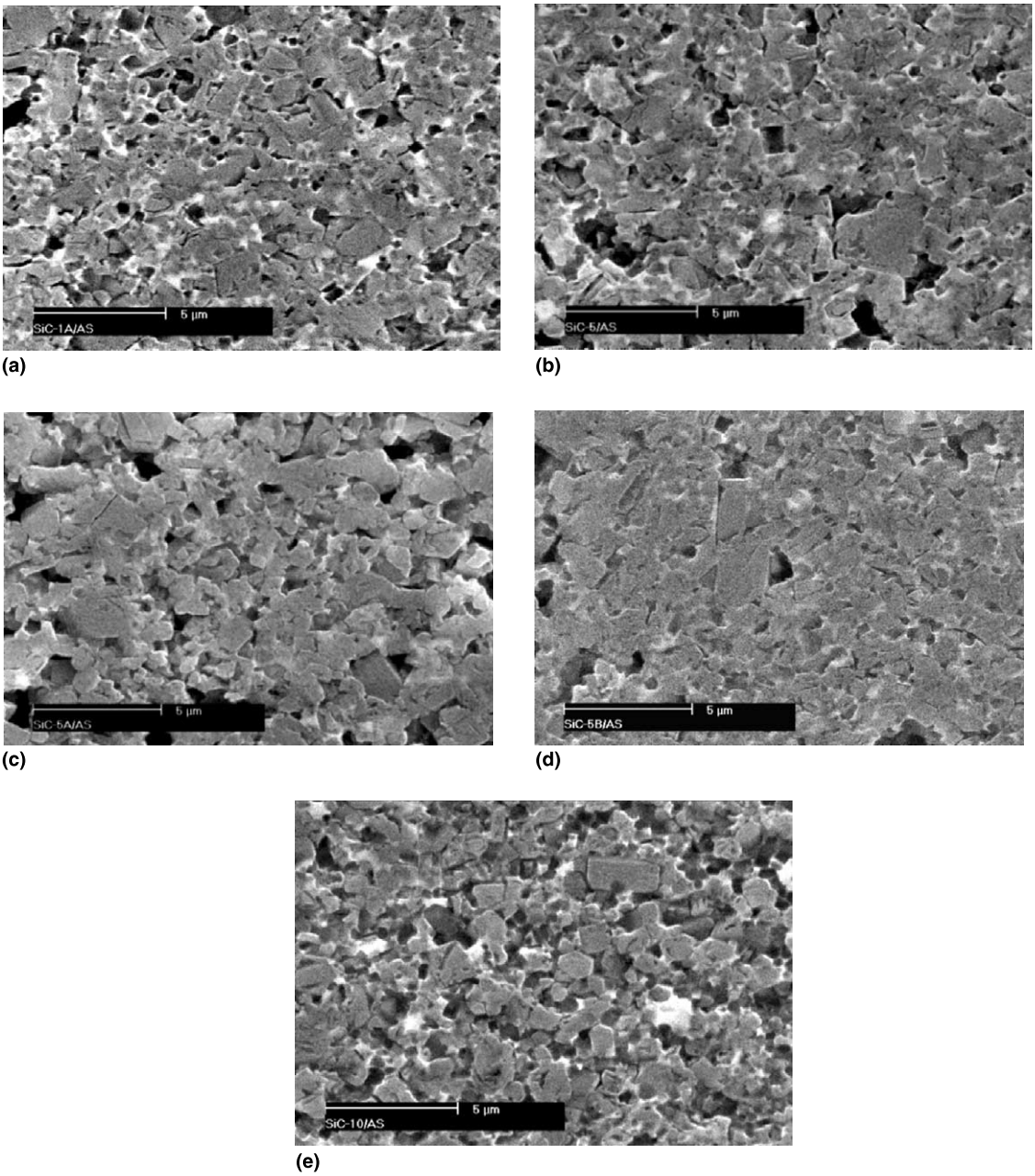

Fig. 6. Microstructure of polished and chemically etched as-sintered samples: (a) SiC1A; (b) SiC5; (c) SiC5A; (d) SiC5B; (e) SiC10.

nitrogen [10,11] while others, including the present authors, report argon atmosphere as a more effective one [6–8,12]. In the present work, both sintering and post-sintering heat treatments were carried out in argon, however an investigation of a post-sintering heat treatment in nitrogen, according to Rixecker et al. [11], may provide interesting results as well. Considering the preferable dissolution of nitrogen in alumosilicate melts as compared to the dissolution of SiC, nitrogen atmosphere may strongly influence both the phase transformation kinetics and the thermal dissociation and volatile product formation during prolonged high-temperature annealings. The gas pressure during post-sintering heat treatment may also be of strong influence. Investigation in this direction is under way at present time.

The results of XRD investigations of the transformation kinetics are in good agreement with the microstructural observations, the latter confirming the possibility of LPS–SiC final microstructure tailoring by control of α/β ratio in the starting compositions, and by additional heat treatment of sintered materials. The results of SEM investigations of polished and chemically etched sintered and annealed samples are presented in Figs. 6 and 7. From these results it could be concluded

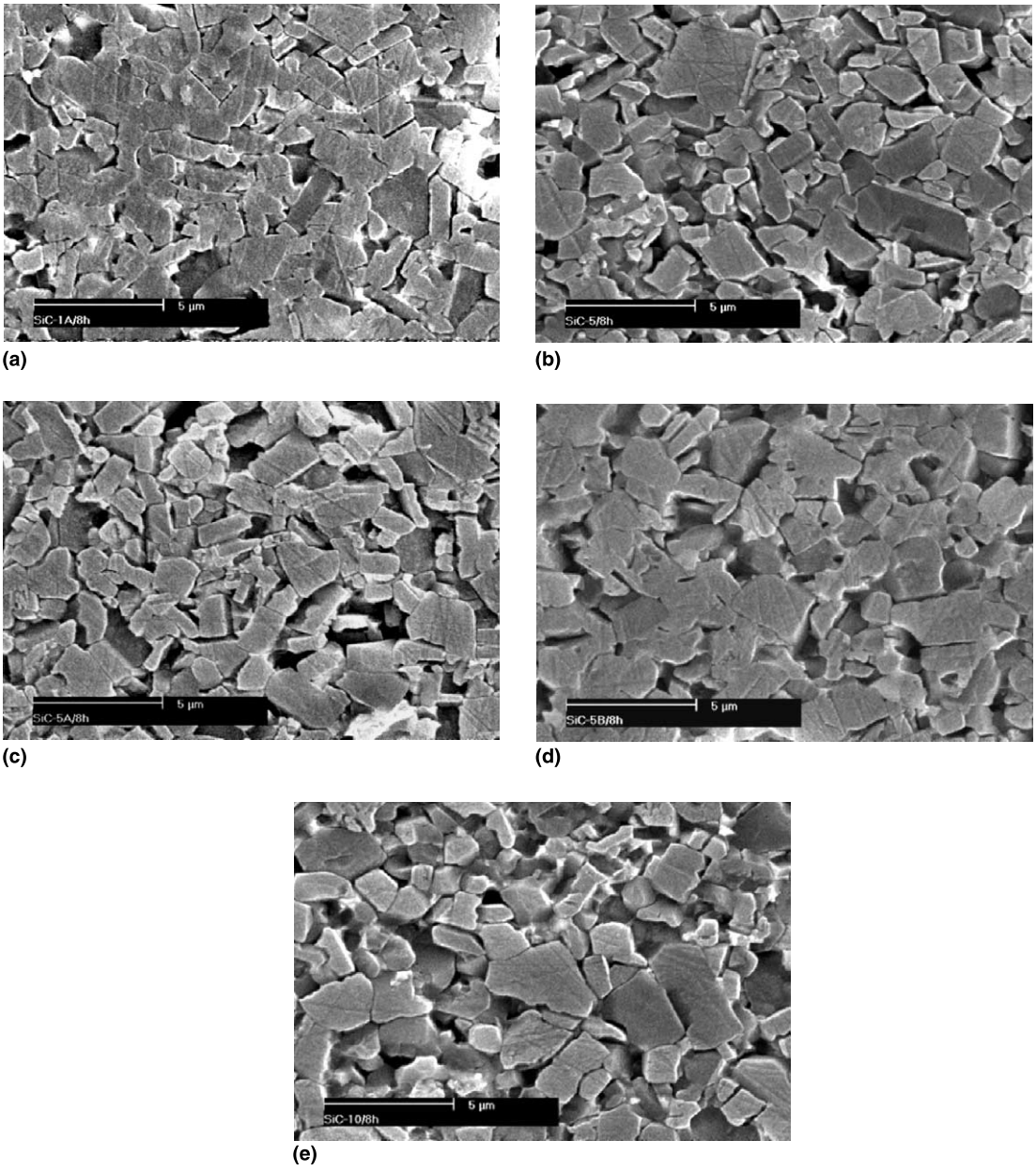

Fig. 7. Microstructure of polished and chemically etched samples after 8 h of annealing at 1950°C in Ar: (a) SiC1A; (b) SiC5; (c) SiC5A; (d) SiC5B; (e) SiC10.

that a significant change of the grain morphology could be obtained due to phase transformation. Since transformation is relatively slow, the formation of elongated grains with a plate-like morphology requires long sintering times.

As it was pointed out earlier, the density of α-SiC nuclei strongly influences the transformation kinetics and therefore microstructure evolution. In the case of a low α-SiC nuclei density, only a limited number of particles will be able to grow. Moreover, these grains should be able to grow during extended sintering times with only a minor steric impediment resulting in an increasing aspect ratio of these grains. This assumption is supported by the observed difference between the microstructure of annealed samples containing 1% and 10% of α-SiC in the initial mixture (see Figs. 7(a) and (e)). The former microstructure is more fine, and has a more pronounced plate-like morphology than the latter, which is coarser and has a grain structure with lower aspect ratios. The influence of the granulometry of α-SiC additions can be seen from the comparison of the microstructure morphology of the annealed samples SiC5, SiC5A, and SiC5B (Figs. 7(b), (c), and (d)). The finer α-SiC powder additives yield a more homogeneous microstructure with higher amount of fine plate-like grains, while the coarser α-SiC additions result in a coarser, less homogeneous microstructure with lower overall amount of plate-like grains, which are sufficiently bigger than in the former material. This effect is directly related with the number and size of α-SiC nuclei in the initial mixtures. Thus, controlling both the amount and the particle size of α-SiC additions provides excellent possibilities for microstructure tailoring of LPS–SiC. The difference between the microstructures of as-sintered materials with varying amount and granulometry of α-SiC additions is less pronounced, however the trend observed for thermally treated materials is similar (Fig. 6).

The opportunity to control the microstructure evolution by introducing into the initial mixture varying amounts of additions which further serve as nuclei for transformation-controlled grain growth is similar to that in case of Si_3N_4 ceramics [21]. However, the resulting grain morphology differs between both materials: Si_3N_4 grains have needle-like morphology due to a high growth rate of the basal planes as compared to the prism planes, whereas in case of SiC the prism planes grow faster than the basal ones, and the grain morphology is plate-like.

The structure of LPS–SiC may be described as consisting of two main components: SiC grains, and an intergranular secondary phase, amorphous or partly crystalline. According to the EDS results, the secondary intergranular phase is an alumosilicate enriched with Y_2O_3, and is assumed to be weaker than the SiC grains. Therefore, an intergranular fracture mode should be a predominant one in the investigated materials. The crack path and the energy required for crack propagation in such a case will be influenced by the size and the morphology of the grains, which is consistent with the results of the fracture toughness measurements (Fig. 8), and the SEM observations of crack propagation in as-sintered and annealed materials (Fig. 9). A general trend of fracture toughness increasing with the increase of the degree of β-SiC to α-SiC transformation and the resulting growth of elongated plate-like grains during post-sintering heat treatment has been observed. The toughening of the materials is attributed to crack deflection, crack bridging, and occasional grain pull-out. The positive effect of microstructure development resulting from anisotropic grain growth is to some extent diminished by the increase of residual porosity due to materials thermo-chemical decomposition during post-sintering heat treatment. After 16 h of annealing at 1950°C under normal Ar pressure, weight loss increased up to 12–14%, as compared to 2.5–3.5% after initial sintering, which led to respective residual porosity increase from 1.2–2.3% to 7–8.5%. This effect also complicates the interpretation of the α-SiC additions amount and type influence on materials' final properties, since weight loss appears to be influenced by them as well. Obviously, the post-sintering heat treatment parameters must be optimized in order to achieve the desirable microstructure without causing density degradation. In this regard both temperature and gas pressure seem to be of main interest. The hardness of the investigated materials exhibited steady decrease with the increase of the post-sintering heat treatment time (Fig. 10), obviously due to the increase of porosity observed for all heat treated samples. Therefore it is assumed that the mechanical properties could be significantly improved by processing conditions and sintering and post-sintering heat treatment parameters' optimization.

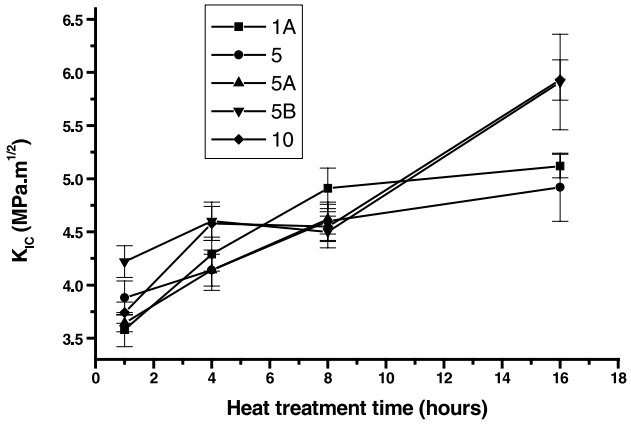

Fig. 8. Indentation fracture toughness as a function of heat treatment time at 1950°C under atmospheric argon pressure.

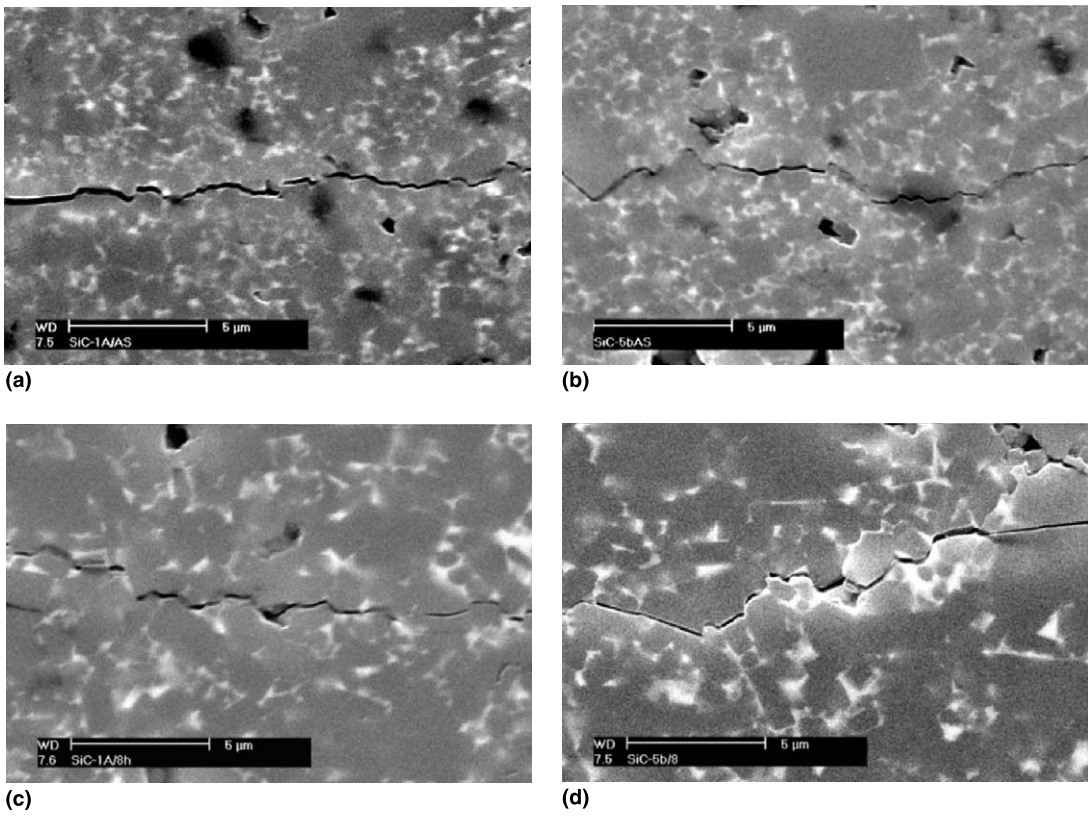

Fig. 9. SEM micrographs of crack propagation in: (a) as-sintered (1 h at 1950°C under atmospheric argon pressure) and (b) heat treated samples (8 h at 1950°C under atmospheric argon pressure).

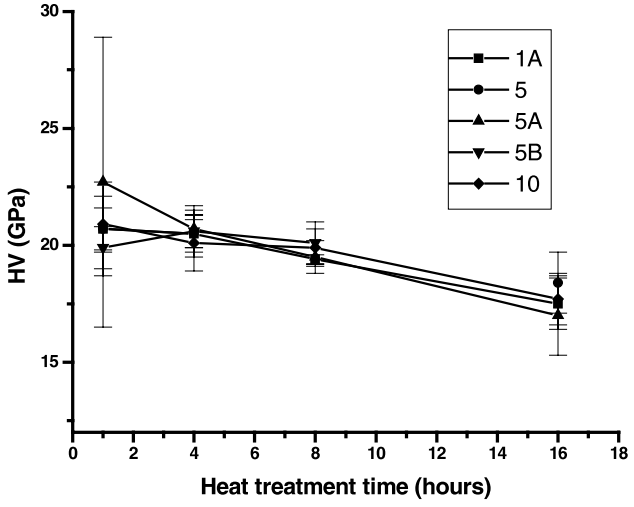

Fig. 10. Vickers hardness as a function of heat treatment time at 1950°C under atmospheric argon pressure.

4. Conclusions

A thorough investigation of the β-SiC to α-SiC phase transformation kinetics and the corresponding microstructural evolution of liquid phase sintered SiC carried out in the present work indicates that the transformation rate is controlled by the number of α-SiC nucleation sites as well as by the sintering and post-sintering time and temperature. The transformation kinetics are relatively slow so that heat treatments of more than 8 h at 1950°C are required to achieve sufficient degree of transformation. The phase transformation can be used for microstructure and microstructure-sensitive properties tailoring of LPS–SiC ceramics due to anisotropic grain growth behavior of SiC resulting in in situ grown plate-like grain morphology. The latter is shown to sufficiently improve the fracture toughness of the investigated materials. However, further optimization of processing and heat treatment of this group of materials in order to avoid density degradation is necessary.

Acknowledgements

The authors would like to express their gratitude to CNPq for the financial support of Dr. V. Izhevskyi's participation in this research. Present research is supported by PRONEX/FINEP, and by FAPESP project 00/07717-8.

References

[1] Cutler RA, Jackson TB. Liquid phase sintered silicon carbide. In: Tennery VJ, editor. Ceramic materials and components for engines, Proceedings of the Third International Symposium. Westerwille, OH: American Ceramic Society; 1989. p. 309–18.

[2] Mulla MA, Krstic VD. Low-temperature pressureless sintering of β-silicon carbide with aluminum oxide and yttrium oxide additions. Am Ceram Soc Bull 1991;70:439–43.

[3] Mulla MA, Krstic VD. Pressureless sintering of β-SiC with Al_2O_3 additions. J Mater Sci 1994;29:934–8.

[4] Lee SK, Kim CH. Effects of α-SiC versus β-SiC starting powders on microstructure and fracture toughness of SiC sintered with Al_2O_3–Y_2O_3 additives. J Am Ceram Soc 1994;77:1655–8.

[5] Omori M, Takei H. Pressureless sintering of SiC. J Am Ceram Soc 1982;65:C92.

[6] Padture NP. In-situ toughened silicon carbide. J Am Ceram Soc 1994;77:519–23.

[7] Padture NP, Lawn BR. Toughness properties of a silicon carbide with in-situ induced heterogeneous grain structure. J Am Ceram Soc 1994;77:2518–22.

[8] Kim WJ, Kim Y-W. Liquid-phase sintering of silicon carbide. J Kor Ceram Soc 1995;32:1162–8.

[9] Chia KY, Boecker WDG, Storm RS. Silicon carbide bodies having high toughness and fracture resistance and method of making same. United States Patent, 5. 298. 470, USA, 1994.

[10] Keppeler M, Reichert H-G, Broadly JM, Turn G, Wiedmann I, Aldinger F. High temperature mechanical behavior of liquid phase sintered silicon carbide. J Eur Ceram Soc 1998;18:521–6.

[11] Rixecker G, Biswas K, Wiedmann I, Aldinger F. Liquid-phase sintered SiC ceramics with oxynitride additives. J Ceram Proc Res 2000;1:12–9.

[12] Izhevskyi VA, Genova LA, Bressiani AHA, Bressiani JC. Liquid phase sintered SiC. Processing and transformation controlled microstructure tailoring. Mater Res 2000;3:131–8.

[13] Izhevskyi VA, Genova LA, Bressiani JC, Bressiani AHA. Liquid-phase sintering of SiC-based ceramics. Key Eng Mater 2001;189–191:173–80.

[14] Nader M, Aldinger F, Hoffmann MJ. Influence of the α/β-SiC ohase transformation on microstructural development and mechanical prperties of liqiud phase sintered silicon carbide. J Mater Sci 1999;34:1197–204.

[15] Moberlychan WJ, Cao JJ, De LC. The roles of amorphous grain boundaries and the β–α transformation in toughening SiC. Acta Mater 1998;46:1625–35.

[16] Becher PF, Hsueh C, Angelini P, Tiegs TN. Toughening behavior in whisker-reinforced ceramic-matrix composites. J Am Ceram Soc 1998;71:1050–61.

[17] Faber KT, Evans AG. Crack deflection process – I. Theory Acta Metall 1983;31:565–76.

[18] Jeutter A. Untersuchung der Phasenbeziung im Sysytem Aluminiumnitrid-Yttriumoxid. Diplomarbeit an Universitat Stuttgart; 1993.

[19] Anstis GR, Chantikul P, Lawn BR, Marshall DB. A critical evaluation of indentation techniques for measuring fracture toughness: I. Direct crack measurements. J Am Ceram Soc 1981;64:533–8.

[20] Christian JW. Phase transformations in metals. New York: Pergamon Press; 1965.

[21] Krämer M, Hoffmann MJ, Petzow G. Grain growth kinetics of Si_3N_4 during α/β transformation. Acta Metall Mater 1993;41:2939–47.

[22] Sajgalik P, Glausek D. α/β transformation of silicon nitride: homogeneous and heterogeneous nucleation. J Mater Sci 1993;12:1937–9.

[23] Wallace JS, Kelly JF. Grain growth in Si_3N_4. Key Eng Mater 1994;89–91:501–5.

[24] Ordonez S, Iturriza I, Castro F. The influence of amount and type of additives on $\alpha \rightarrow \beta$ Si_3N_4 transformation. J Mater Sci 1999;34:147–53.